

The effect of the processing parameters on the fabrication of auxetic polyethylene

Part I *The effect of compaction conditions*

A. P. PICKLES, R. S. WEBBER, K. L. ALDERSON, P. J. NEALE

Department of Materials Science and Engineering, The University of Liverpool, PO Box 147, Liverpool L69 3BX, UK

K. E. EVANS*

School of Engineering, University of Exeter, North Park Road, Exeter EX4 4QF, UK

A novel fibrillated particulate microstructure has been fabricated in ultra high molecular weight polyethylene (UHMWPE) that produces a negative Poisson's ratio (auxetic) material. The processing route involves compaction, sintering and extrusion of a UHMWPE fine powder. The first, compaction stage is examined in this paper in detail in order to ascertain the compaction conditions required to produce, as an end-product, an auxetic polymer and to assess the importance of this stage in the processing route. It was found that while part of the function of the compaction stage was to impart structural integrity to the processed polymers, the conditions for optimizing the production of auxetic UHMWPE were not identical to those for optimum structural integrity of the compact. Both sets of conditions were examined, with compaction pressure and temperature being the most important of the variables examined.

1. Introduction

The fabrication of a microporous form of ultra high molecular weight polyethylene (UHMWPE) which possesses a negative Poisson's ratio (ν) was first reported in 1992 [1]. This auxetic material, in common with a microporous form of polytetrafluoroethylene (PTFE) [2, 3], achieves a negative Poisson's ratio by means of its microstructure which consists of an interconnected network of nodules and fibrils. When the material is deformed in tension, the nodules and fibrils react co-operatively to produce an expansion in the transverse direction with the fibrils causing the nodules to be pushed apart. In order to produce the auxetic form of UHMWPE, a novel thermal processing route was developed [1, 4] consisting of 3 distinct stages: compaction, sintering and extrusion of a fine powder of UHMWPE.

An initial set of conditions for the production of UHMWPE which combines an acceptable structural integrity (i.e. a modulus of at least 0.2 GPa [5]) and the property of being auxetic have been determined [1, 4]. The process commences with the compaction stage, which takes place within the barrel of a specially designed rig fitted with a blank die (see Fig. 1(a)). The internal dimensions of the barrel were a bore diameter of 10 mm and a length of approximately 90 mm. For convenience, these will be referred to as the standard conditions. Finely divided UHMWPE powder (supplied by Hoechst [6]) was poured into the barrel,

which was at a preset temperature of 110 °C and left to equilibrate for a period of 10 min (referred to as the stand time). After this, compaction was achieved by lowering the brass tipped ram into the powder at a rate of 20 mm min⁻¹ (the loading rate) until an applied pressure of 0.04 GPa had been achieved, with the load being applied via the ram which was attached to the load cell of a Schenk–Trebel electro-mechanical testing machine for 20 min, with fluctuations between 0.041 and 0.037 GPa as the powder settled. After 20 min loading time, the load was removed and the compacted rod pushed out of the barrel.

After it had been allowed to slowly cool to room temperature, the compacted rod was reinserted into the barrel, which was now at a preset temperature of 160 °C. The same rig was used as in the compaction stage of the processing route, except that the blank die was replaced with a die of exit diameter 5 mm, cone semi-angle of 30° and capillary of 3.4 mm (see Fig. 1(b)). After 20 min sintering, extrusion took place at a rate of 500 mm min⁻¹, again at a temperature of 160 °C.

In this new work, the conditions necessary to make auxetic UHMWPE of larger dimensions (i.e. the diameter of the barrel was increased to 15 mm, the barrel length to 165 mm and the exit diameter of the die to 7.5 mm) and the effects of varying the processing conditions away from the standard case were explored. In particular, interest centred on achieving structural

* Author to whom correspondence should be addressed.

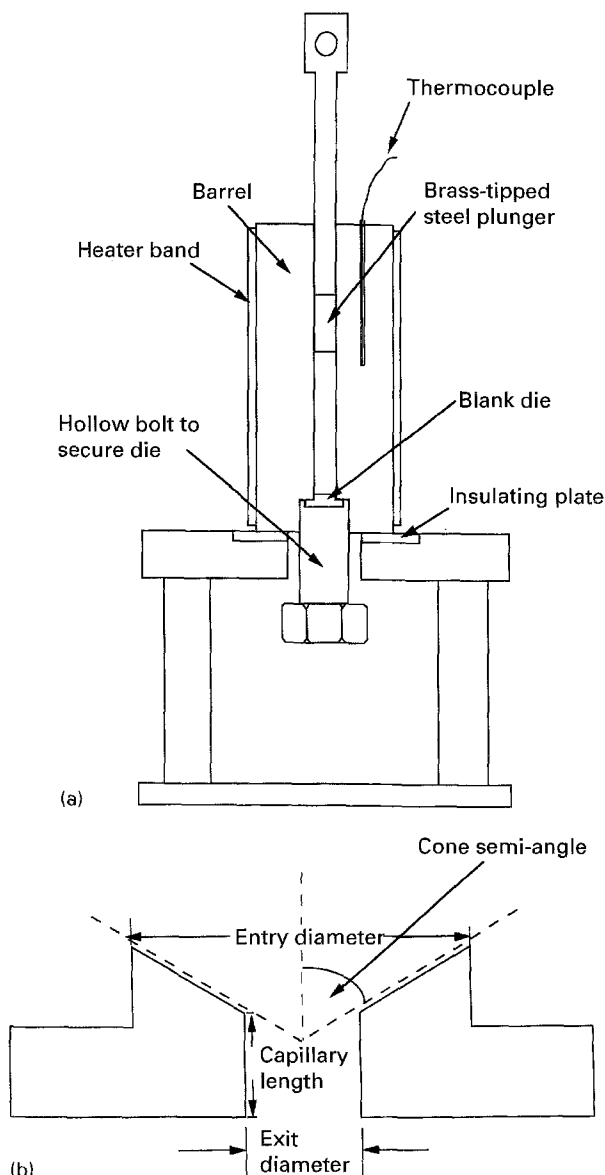


Figure 1 (a) Schematic of the rig used in the fabrication process, (b) schematic of a standard die.

integrity of the extrudate and obtaining a range of Poisson's ratio. This paper forms part of a series [7, 8] which studies in detail the effects of varying the processing parameters within each stage of the fabrication route and concentrates on providing a greater understanding of the first stage of the processing route, i.e. compaction of finely divided UHMWPE powder to produce rods for further processing.

The room temperature (or cold) compaction process for conventional polymers is well documented and understood [9–11]. Crawford and Paul [9] explain the compaction process as occurring in a number of distinct stages. On filling a chamber, the powder particles fall into a random arrangement and hold each other in position by the formation of arches and bridges between adjacent particles and by friction between particles and the chamber wall. The density of the powder at this point is the lowest achievable and is referred to as the bulk density. As the powder is compacted, the applied pressure causes the bridging to be destroyed and the particles move to a lower position. From powder metallurgy, this stage is known to

have an influence on the subsequent transmission of pressure through the powder. Further compaction results in the elastic deformation of particles at their contact points with other particles or the walls of the container. This elastic deformation allows further rearrangement of particles, with smaller particles moving to fill the gaps between larger particles. As the load increases, plastic deformation occurs, leading to a large reduction in porosity.

This investigation examines the effects of varying the compaction conditions on the microstructure, density, mechanical properties and ability of the rods produced to form an auxetic polymer. The primary function of compaction in this processing route is to impart some degree of structural integrity to the rods without (unlike conventional compaction) excessively reducing porosity. Hot compaction is necessary to aid structural integrity, normally obtained by the higher pressures of cold compaction. So it is expected that the requirements for the compaction stage of this process will be very different from those of previous work where the aim was a highly compacted end-product.

2. Experimental methods

The polymer used in this study was GUR 415 UHMWPE powder supplied by Hoechst [6] and its powder morphology is shown in Fig. 2. The barrel of the processing rig was heated by an external band heater, with the temperature being controlled by a thermocouple placed within the barrel wall (see Fig. 1(a)). Precise calibration of the rig (and indeed of all barrel and bore sizes used to date) has been carried out by placing a second thermocouple in the powder in the bore and comparing the temperature it records with that displayed by the thermocouple sited in the barrel wall. It was found that the temperature of the powder was within 2% of that recorded by the thermocouple in the barrel wall up to the required sintering temperature of 160 °C and beyond for all combinations of barrel and bore size used to date. In the example shown in Fig. 3, for the barrel and bore size used in this part of the investigation (i.e. a barrel of length 165 mm and bore diameter 15 mm), agreement within 0.1 °C was seen between the two thermocouples.

A typical schematic load against time trace obtained during compaction is shown in Fig. 4. This shows the stand time (under zero load), the compaction stage (where the load gradually increases at first followed by a rapid increase) and the loading time (where the load is maintained around the desired value).

2.1. Variables investigated in the compaction stage of the fabrication route

The starting point for this work was the set of standard conditions previously found to achieve auxetic properties in a smaller barrel geometry [1, 4] as detailed in the Section 1. In order to investigate the effects of each of the five variables in turn, one variable at a time was changed with the other four remaining

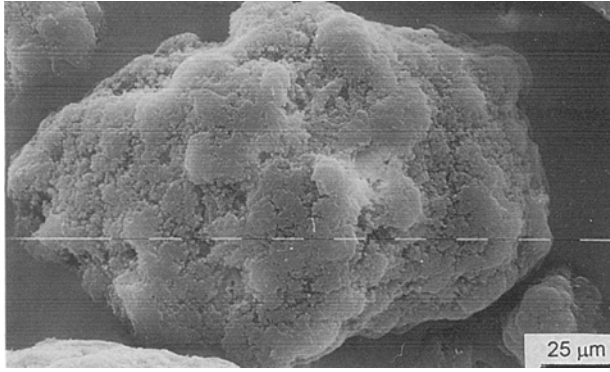


Figure 2 Micrograph of the polymer powder.

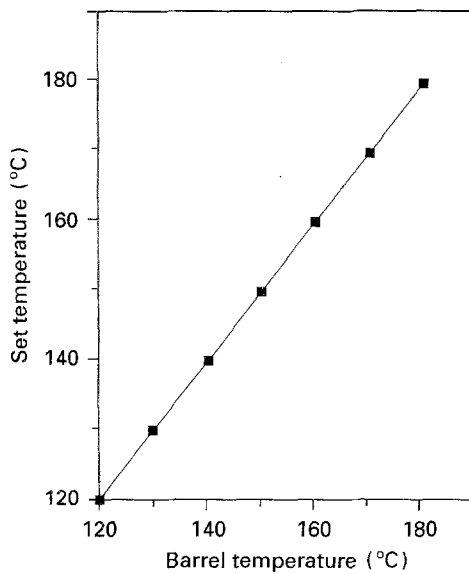


Figure 3 Temperature calibration curve for the barrel of length 165 mm and bore diameter 15 mm used in this investigation.

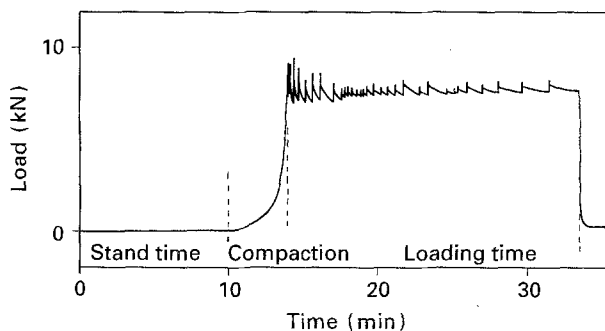


Figure 4 Graph of load against time for the compaction process, indicating the variation of load as the compaction process goes through the various stages.

as standard. The stand times investigated were 0, 5, 10, 15, 20 and 40 min. Loading rates were 1, 5, 10, 20, 40 and 80 mm min⁻¹ up to pressures of 0.005, 0.011, 0.022, 0.040, 0.082 and 0.164 GPa. The pressure was held for times of 1, 5, 10, 20, 40 and 80 min and the barrel temperature was set at 80, 95, 110, 125, 133, 140

and 155 °C. The temperature of 133 °C was selected as this is the mid-temperature in the quoted crystalline melting range, which is 130–135 °C [12]. However, it should be noted that even at 190 °C, experiment has shown that the polymer is not fully molten, rather it has softened as a result of its very high molecular weight.

It was not possible to achieve in practice a zero stand time because of the time needed to charge the barrel and set the ram in position before compaction could commence. The shortest stand time obtainable was found to be approximately 1 min.

2.2. Examination of the compacted rods

After compaction was completed, the rod was pushed from the barrel and examined. An initial visual assessment was made to note any obvious differences and the degree of compaction was examined by measuring the density of the rods. Mechanical property data were obtained by performing a 3-point bend test. A span equal to five times the diameter of the rod was used in accordance with a British Standard [13]. Although not strictly applicable, the test is justified on the basis that it provides data which can be used to examine variations with respect to the different compaction conditions. The 3-point bend test provided information on the flexural strength, modulus and strain which were calculated using the equations below

$$\text{Flexural strength, } S = \frac{8PL}{\pi D^3} \quad (1)$$

$$\text{Flexural modulus, } E = \frac{4PL^3}{3\pi D^4 y} \quad (2)$$

$$\text{Flexural strain at failure, } \varepsilon = \frac{6Dy}{L^2} \quad (3)$$

where P is the load at failure, L the support separation, D the rod diameter and y the maximum rod deflection at failure [14]. The majority of specimens failed by brittle fracture with a well defined failure point.

The final method of examination was to look at the fracture surfaces produced by the 3-point bend test. A suitable section, consisting of a fracture surface, was taken from each rod, mounted on an aluminium stub and gold coated using an Edwards S150 sputter coater. The coated samples were then examined using a Philips 501 scanning electron microscope (SEM) at magnifications of up to $\times 1250$.

2.3. Sintering and extrusion of compacted rods

As a final stage, some of the rods which had been compacted under certain selected conditions were subjected to standard sintering and extrusion conditions [1, 4], as detailed in Section 1, to evaluate their ability to produce auxetic material. The rods thus produced were subjected to simple compression testing in the radial direction and, using a photographic technique developed in-house [3], the Poisson's ratio

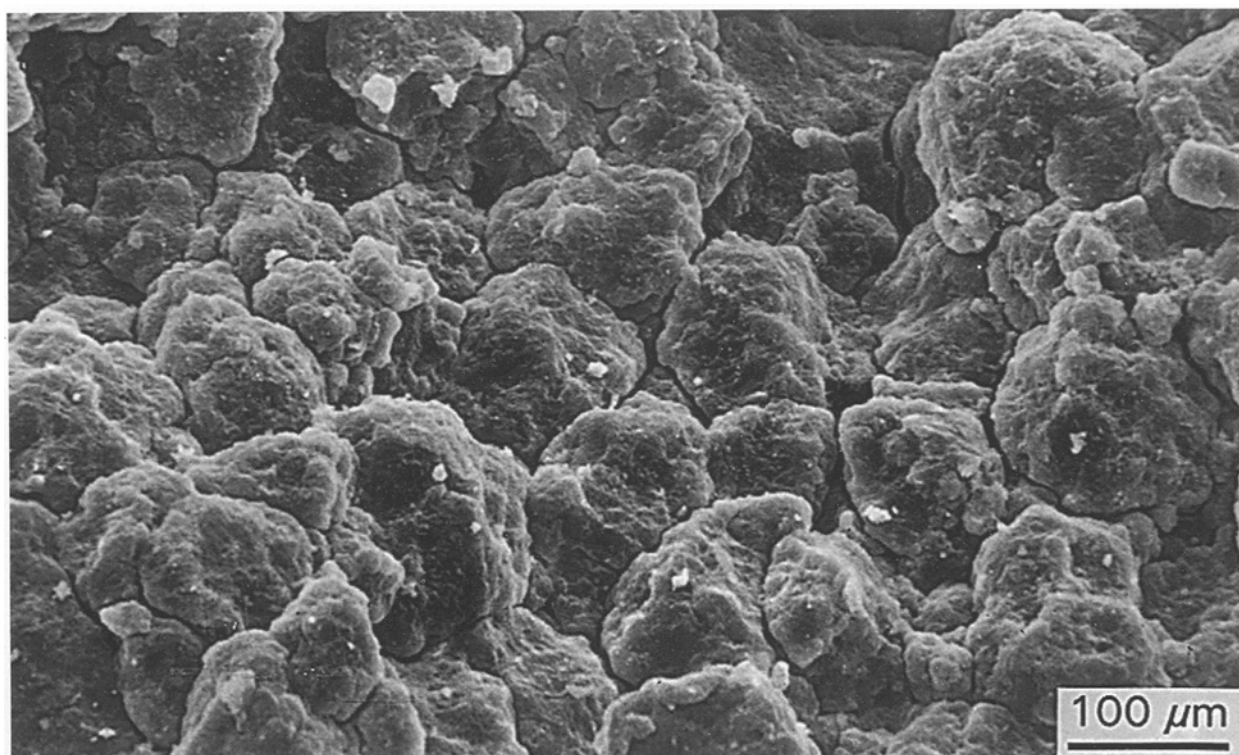


Figure 5 Micrograph of a rod compacted under standard conditions.

TABLE I Values of the 3-point bend data obtained from rods compacted under standard conditions

	Units	Value	Standard deviation
Density	(kg m^{-3})	880	3
Strength	(MPa)	5.2	0.5
Modulus	(MPa)	290	10
Failure strain	(%)	1.8	0.1

was measured. The accuracy of this very simple technique has been verified by the use of electronic resistance strain gauges [15].

3. Results

3.1. Assessment of rods compacted under standard conditions

To assess the consistency, five compacted rods were produced under standard conditions. Fig. 5 shows the fracture surface of one such rod as observed using the SEM. The rods were subjected to density measurements and 3-point bend tests and the results of these

investigations are shown in Table I. It can be seen that the error on the measurements is small, particularly for the properties of density and modulus, indicating that the compacted rods produced are of an acceptable consistency.

3.2. Effect of the variables investigated in the compaction process

The results of investigations into the five variables in the compaction process are considered separately below. Unless specified, all other non-varying conditions were kept at the standard values (as detailed in Section 1).

3.2.1. The effect of stand time

Both visual and SEM examinations of compacted rods produced at the standard (10 min) and extremes (1 and 40 min, respectively) revealed that all specimens produced were of similar physical appearance, microstructure, dimensions and structural integrity. Table II shows the variations of density, strength, modulus and

TABLE II Variation of properties with stand time, with errors as shown in Table I

	Units	Stand time (min)					
		1	5	10	15	20	40
Density	(kg m^{-3})	884	881	884	884	886	876
Strength	(MPa)	6.4	6.1	6.0	6.1	6.3	6.4
Modulus	(MPa)	324	302	299	301	340	317
Failure strain	(%)	2.0	2.0	2.0	2.0	1.9	2.0

TABLE III Variation of properties with loading rate, with errors as shown in Table I

	Units	Loading rate (mm min ⁻¹)					
		1	5	10	20	40	80
Density	(kg m ⁻³)	878	878	883	877	878	880
Strength	(MPa)	5.9	5.4	5.5	4.8	4.4	4.8
Modulus	(MPa)	291	263	272	279	270	266
Failure strain	(%)	2.0	2.1	2.0	1.7	1.6	1.8

TABLE IV Variation of properties with applied pressure, with errors as shown in Table I

	Units	Applied pressure (GPa)					
		0.005	0.011	0.022	0.040	0.082	0.164
Density	(kg m ⁻³)	705	788	849	880	870	878
Strength	(MPa)	1.6	3.9	4.7	4.9	3.8	3.8
Modulus	(MPa)	117	194	239	278	223	263
Failure strain	(%)	1.7	2.0	2.0	1.8	1.7	1.6

strain with stand time, with all other conditions kept as standard. From Table II, it can be seen that densification is relatively unaffected by increasing stand time with the average value of density being $883 \pm 3 \text{ kg m}^{-3}$, which is consistent with the standard rod density of 880 kg m^{-3} . Variation in the properties measured using 3-point bend testing is also slight. Overall, these results show that stand time is of little or no importance in terms of the compactability of rods.

3.2.2. The effect of loading rate

As with the stand time, the loading rate has only a small effect on the properties of the compacted rod (see Table III). The density remains almost constant, whilst the strength, modulus and strain to failure show a slight drop with increasing compaction rate. It is probable that this slight drop in properties is a result of the particles not having sufficient time to move and rearrange their positions in the early stages of compaction, compared to the low compaction rates. This is also supported by the work of Umeya and Hara [16] who found that a slower compaction speed allowed easier sliding between particles and, as a result of this, a better bond between particles.

Since the decrease in compact quality resulting from a change in rate from 20 to 80 mm min⁻¹ was so small, it was decided that the value of compaction rate could be redefined to be much faster than the standard 20 mm min⁻¹ thus far employed. Some work was then carried out using a compaction rate of 140 mm min⁻¹ (see Section 3.3) to investigate the effects of using an even higher compaction rate but the majority of the results given were obtained at a compaction rate of 20 mm min⁻¹.

3.2.3. The effect of applied pressure

Visual examination of the rods compacted using different applied pressures revealed that, generally, the

quality of rods increased markedly with pressure up until about 0.04 GPa, above which no further changes could be detected by the naked eye alone. The most noticeable change in the rods compacted at the lower pressures was in length and surface porosity (also confirmed by SEM examination) as compaction pressure was varied.

The applied pressure also had one of the largest effects on the mechanical properties (see Table IV and Fig. 6). The density gradually increases from 700 kg m^{-3} to of the order of 880 kg m^{-3} at a pressure of 0.04 GPa, after which it remains virtually constant. The values of strength, modulus and strain to failure (the latter being less susceptible to changes in applied pressure) show similar trends, with a large increase as the pressure is increased up to 0.04 GPa. After this, higher pressures appear to result in a drop in properties. The general decrease in mechanical properties may indicate that at higher pressures the particles are being damaged. It is probable that at the higher pressures, considerable plastic deformation will have occurred as well as elastic bulk deformation. When the pressure is removed, the compacted rod is able to recover slightly, and it appears that the deformation process results in less cohesion between particles (observed by SEM examination), leading to a reduction in properties.

3.2.4. The effect of loading time

The time for which the standard 0.04 GPa pressure is applied does have an effect on the properties of the compacted rods (see Table V). A peak in mechanical properties was observed at a loading time of 10 min. After this time, a gradual decrease in properties was obtained, along with an increase in specimen porosity as confirmed by SEM examination. According to the results of Han *et al.* [11, 17], the increase in porosity was probably due to the relaxation of the particles due to the length of time available for the process.

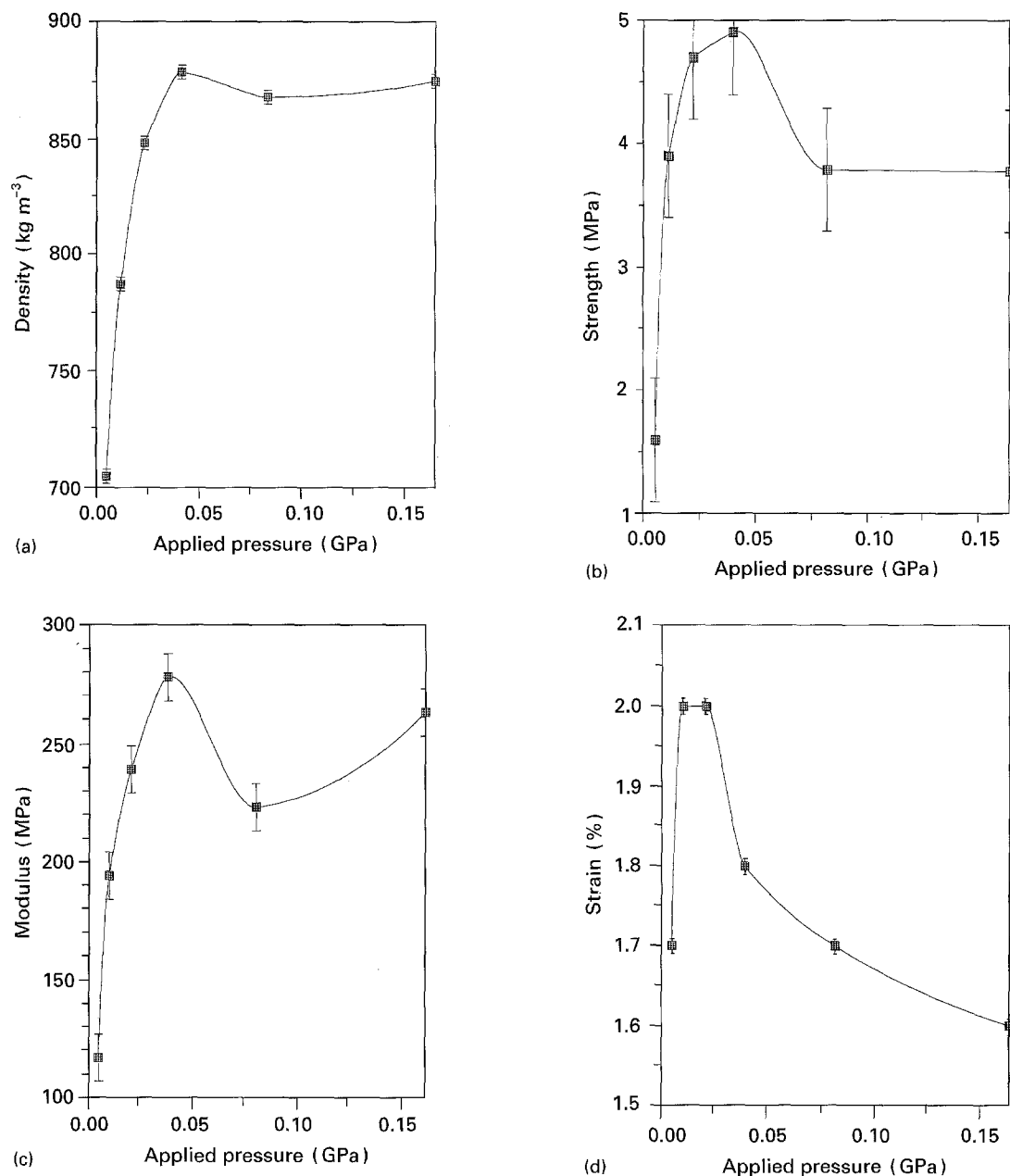


Figure 6 Graph of (a) density, (b) strength, (c) modulus and (d) strain to failure as a function of applied pressure.

TABLE V Variations in properties with loading time, with errors as shown in Table I

	Units	Loading time (min)					
		1	5	10	15	20	40
Density	(kg m ⁻³)	849	860	878	884	892	880
Strength	(MPa)	5.3	5.7	6.5	5.9	6.3	4.9
Modulus	(MPa)	240	266	325	299	318	274
Failure strain	(%)	2.3	2.1	2.0	1.9	2.0	1.8

3.2.5. The effect of compaction temperature

Variation in compaction temperature showed by far the greatest effect on mechanical properties (see Table VI and Fig. 7) and morphology. Figs 8 and 9 show fracture surfaces obtained from samples produced at temperatures of 80 and 140 °C, respectively. It can be seen that the particles of the rod compacted at 80 °C were clearly identifiable, were relatively undeformed and even in regions of intimate contact had not coales-

ced to any great degree. The particles of the rods compacted at 140 °C had, however, coalesced to such an extent that the interparticle boundaries in some regions had disappeared completely. This would appear to indicate that the rods had fully densified around this temperature, which was indeed the case. Fig. 7(a) shows a peak in density of 951 kg m⁻³ at a temperature of 133 °C, which is in agreement with the theoretical maximum density of the order of 950 kg m⁻³.

TABLE VI Variation of properties with compaction temperature, with errors as shown in Table I

		Compaction temperature (°C)						
	Units	80	95	110	125	133	140	155
Density	(kg m ⁻³)	811	858	878	890	951	905	920
Strength	(MPa)	1.6	3.4	5.6	10.5	15.6	29.4	31.5
Modulus	(MPa)	139	235	296	358	428	290	188
Failure strain	(%)	1.1	1.5	1.9	2.9	3.6	10.1	9.5

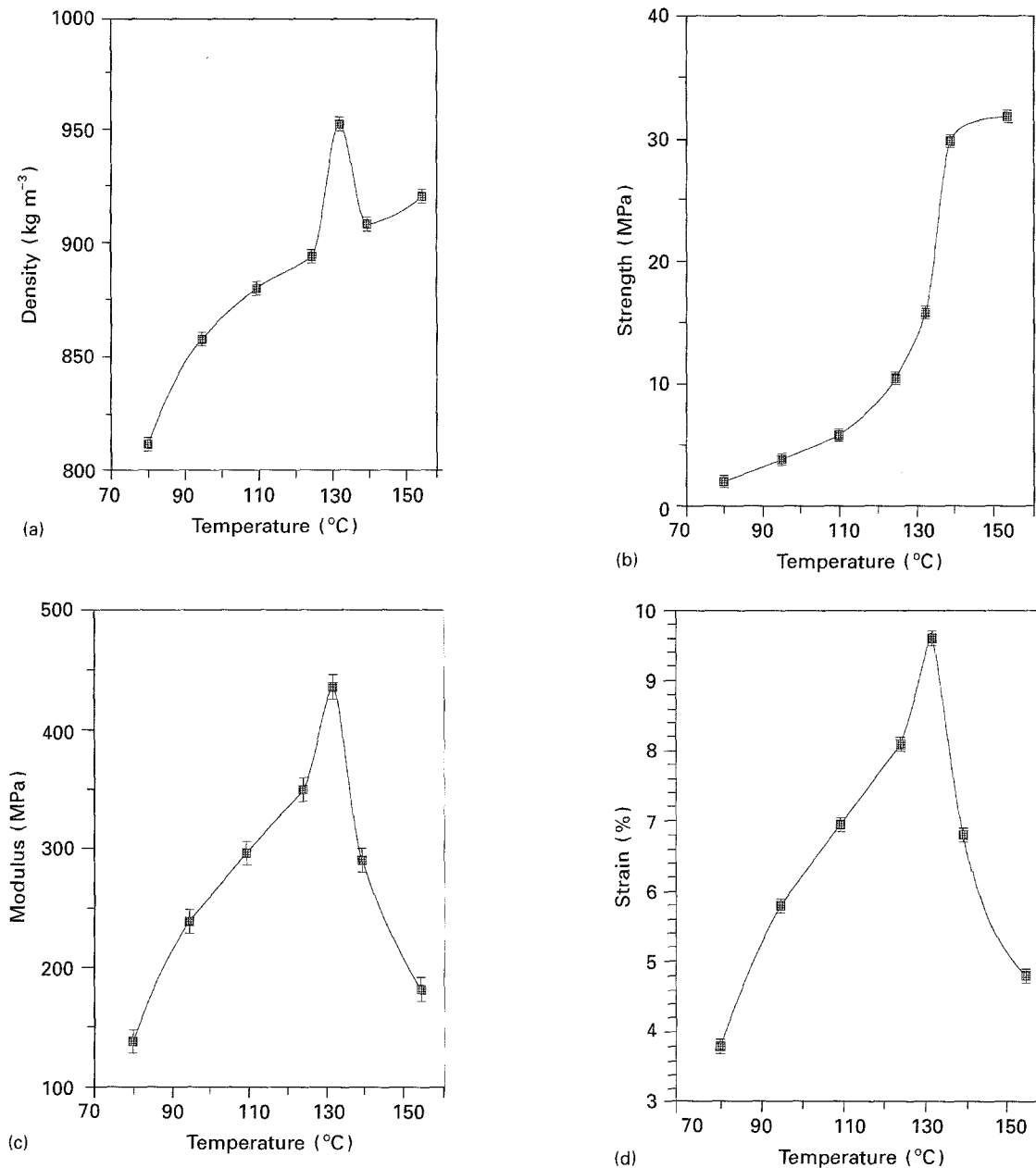


Figure 7 Graph of (a) density, (b) strength, (c) modulus and (d) strain to failure as a function of compaction temperature.

3.3. Sintering and extrusion of compacted rods

Based on the results of the densification measurements, visual and SEM examination and mechanical property testing, rods produced under selected compaction conditions were prepared and subjected to standard sintering and extrusion conditions as detailed above. The extrudates thus produced were

tested in compression to measure their Poisson's ratio to ascertain the effects of compaction on the ability of the rods to form auxetic material. It was found that the compaction conditions do have a very definite effect besides that of imparting structural integrity, which remains one of the primary functions of this stage in the processing route. Specimens compacted under standard conditions do produce auxetic mater-

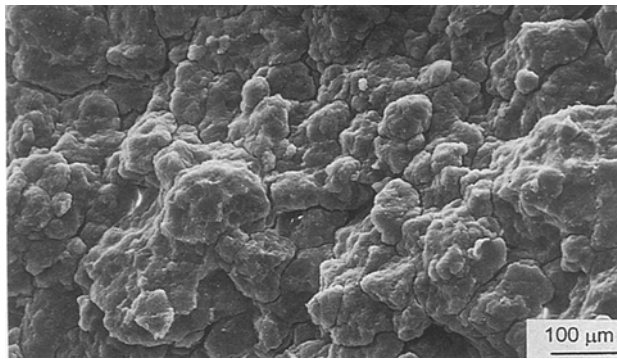


Figure 8 Micrograph of a compacted rod produced at a temperature of 80 °C.

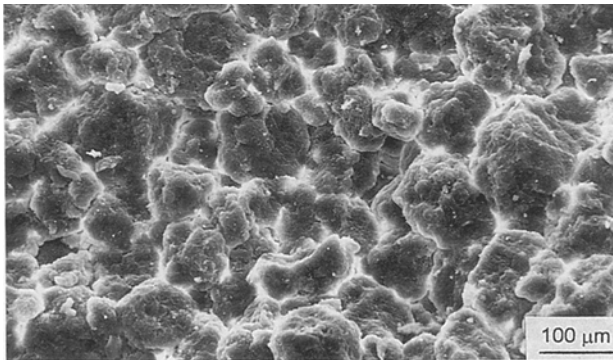


Figure 9 Micrograph of a compacted rod produced at a temperature of 140 °C.

TABLE VII Radial Poisson's ratio values measured in compression for rods compacted at a temperature of 110 °C, after a stand time of 10 min, with a loading rate of 20 mm min⁻¹ at a pressure of 0.04 GPa for a loading time of 20 min. Each result is for a separate sample and the error on the radial Poisson's ratio is ± 0.02

Compressive strain	Radial Poisson's ratio
0.003	- 0.75
0.010	- 1.52
0.010	0.00
0.010	0.00
0.010	- 0.67
0.011	- 1.45
0.011	+ 2.90
0.011	- 0.54

ial, but variations in compaction conditions also allow for auxetic material to form (see Tables VII and VIII). This will be discussed in detail below.

However, it should be stated that results also revealed that certain compaction conditions do not produce, under standard sintering and extrusion conditions, an auxetic material. Rods compacted at

TABLE VIII Radial Poisson's ratio values measured in compression for rods compacted at a temperature of 125 °C, after a stand time of 3 min, with a loading rate of 140 mm min⁻¹ at a pressure of 0.04 GPa for a loading time of 10 min. Each result is for a separate sample and the error on the radial Poisson's ratio is ± 0.02

Compressive strain	Radial Poisson's ratio
0.003	+ 0.76
0.003	- 0.77
0.003	- 0.38
0.006	- 0.79
0.006	- 1.50
0.011	- 0.60
0.011	- 0.28

TABLE IX Radial Poisson's ratio values measured in compression for rods compacted at a temperature of 155 °C, after a stand time of 40 min, with a loading rate of 80 mm min⁻¹ at a pressure of 0.164 GPa for a loading time of 80 min. Each result is for a separate sample and the error on the radial Poisson's ratio is ± 0.02

Compressive strain	Radial Poisson's ratio
0.052	+ 0.57
0.053	+ 0.17
0.060	0.00
0.064	+ 0.37
0.064	+ 0.62
0.064	+ 1.42
0.065	+ 0.76
0.070	+ 1.42

above 125 °C, at high applied pressures and after subsequent sintering and immediate extrusion did not yield auxetic material, but rather produced positive Poisson's ratio material (see Table IX). Also, below temperatures of 110 °C and at low pressures, the material was almost entirely lacking in structural integrity. In all cases, there is a considerable variation of Poisson's ratio with strain, a characteristic feature of this auxetic material that has been previously described [18].

4. Discussion

The full conclusions concerning optimum compaction conditions to produce auxetic polyethylene cannot be drawn until sintering and extrusion have also been considered in detail. However, at this stage certain compaction conditions can be eliminated.

In conventional polymer processing, the aim of the compaction process is usually to achieve the best possible densification. For this investigation, clearly the most important variables in the compaction process to achieve these ends are applied pressure and temperature. For optimum mechanical properties and density, a compaction pressure of around 0.04 GPa is required (see Table IV and Fig. 6). Compaction for conventional processing is usually carried out at room temperature and it is expected that at the higher temperatures investigated here the additional mechanism of sintering will play a large part in the actual specimen response and morphology. Sintering alone is

a vital stage in the processing route to produce UHMWPE with a negative ν and as such is discussed in detail in a subsequent paper [7] but it should be noted that sintering is occurring in tandem with compaction in this investigation at the higher temperatures. From Fig. 7 and Table VI, it can be seen that the mechanical properties increased with temperature up to 133 °C above which they remained constant or fell slightly. If the end requirement was a compacted, well densified rod, then the temperature selected for processing would be 133 °C.

Regarding the other three variables investigated, the following conclusions can be drawn. Stand time and loading rate have no effect on the quality of rods produced within the wide range of variables considered here, indicating that the optimum conditions for compaction should be as short a stand time and as fast a loading rate as is obtainable safely with the current experimental set up incorporating a blank die. This would mean a stand time of 3 minutes (allowing the charging of the barrel and setting up of the ram to be carried out manually) and a loading rate of 140 mm min⁻¹. As far as loading time is concerned, this is acknowledged as not being the most significant of the compaction variables under investigation, but an optimum loading time for the powder of 10 min can be defined. Thus, it has been possible from this investigation to define for this particular experimental configuration (i.e. polymer powder used, compaction rig available etc.) a set of conditions which would lead to a conventional well densified compacted rod. These are summarised in Table X.

However, the aim of this investigation was not to define a set of processing conditions to produce well-densified rods but rather to define the parameters which would produce, after sintering and extrusion, an auxetic end-product. It was expected from previous work that one of the primary functions of this part of the processing route would be the imparting of structural integrity to the specimens and this was indeed the case. However, if too high a temperature (above 125 °C) or applied pressure (above 0.04 GPa) is employed, the material forms a too highly densified solid rod which cannot be transformed to an auxetic form.

Rods were compacted, sintered and extruded using the standard conditions and with the modified compaction conditions as shown in Table X. It was found that in both cases, rods with a sufficient degree of structural integrity were obtained and that both materials were auxetic. Indeed for the revised compaction conditions, the characteristic strain dependency of Poisson's ratio was readily obtained, with ν as low as -1.5 measured at very low strains (see Table VIII). This is in agreement with previous work [15, 18]. This indicates that there is a well defined range of compaction conditions which can be employed to produce auxetic UHMWPE, and has an important consequence as far as increasing the productivity of compacted rods as a precursor to the formation of auxetic rods under standard sintering and extrusion conditions. Comparing the standard and revised compaction conditions, it can be seen that applied pressure

TABLE X List of compaction conditions (a) previously defined as standard for the production of auxetic UHMWPE, (b) revised in accordance with this investigation and (c) optimum for mechanical performance of compacts

	(a) Standard	(b) Revised	(c) Mechanical
Temperature (°C)	110	110–125	133
Stand time (min)	10	3–10	3
Loading rate (mm min ⁻¹)	20	20–140	140
Pressure (GPa)	0.04	0.04	0.04
Loading time (min)	20	10–20	10

should always be around 0.04 GPa with too low a pressure resulting in a severe loss of structural integrity and too high a pressure in the deformation of particles. The temperature can range from 110 °C to 125 °C without losing the ability of the rods to form auxetic material. As stated previously, stand time is of little or no importance in terms of compactibility, thus allowing compaction to be carried out after as short a stand time as is practical, this being 3 min for this experimental configuration, which is a significant reduction from the 10 min originally recommended. A further reduction in processing cycle time can be obtained by reducing the loading time to the optimum defined in this investigation (i.e. from 20 min to 10 min), with structural integrity maintained. Also, a faster loading rate can be used without any significant detrimental effect to compact quality and ability to form auxetic UHMWPE.

5. Conclusions

By studying the extremes of the compaction process, it can be seen that there is a range of compaction variables within which auxetic material can be formed after standard sintering and extrusion has occurred. The five variables under investigation can be ranked in order of increasing importance as follows: stand time, loading rate, loading time, applied pressure and temperature. With a view to optimizing the compaction conditions, this investigation indicates that stand time and loading time can be substantially reduced and the loading rate increased compared with previous experiments [4]. This significantly reduces the overall time needed to compact a rod and hence increase productivity without any loss in structural integrity or auxetic behaviour of the end-product. Applied compaction pressure and temperature may be left as before, i.e. at 0.04 GPa and 110 °C, though temperatures as high as 125 °C may be successfully employed. These conditions are not the same as those required for optimum mechanical performance of the compact.

Acknowledgements

The authors wish to acknowledge the financial support of ICI Chemicals and Polymers (APP) and the EPSRC through the provision of a studentship (PJN) and a Research Associateship (KLA). KEE wishes to acknowledge the award of an EPSRC Advanced Fellowship during this work.

References

1. K. L. ALDERSON and K. E. EVANS, *Polymer* **33** (1992) 4435.
2. K. E. EVANS and B. D. CADDOCK, *J. Phys. D: Appl. Phys.* **22** (1989) 1883.
3. B. D. CADDOCK and K. E. EVANS, *ibid.* **22** (1989) 1877.
4. K. E. EVANS and K. L. AINSWORTH, International Patent Publication no. WO91/01210 (1991).
5. K. E. EVANS and K. L. ALDERSON, *J. Mater. Sci. Lett.* **11** (1992) 1721.
6. Hoechst UK Limited, Hoechst House, Salisbury Road, Middlesex TW4 6JH.
7. K. L. ALDERSON, A. P. KETTLE, P. J. NEALE, A. P. PICKLES and K. E. EVANS, *J. Mater. Sci.* **30** (1995).
8. P. J. NEALE, A. P. PICKLES, K. L. ALDERSON and K. E. EVANS, *ibid.* **30** (1995).
9. R. J. CRAWFORD and D. W. PAUL, *ibid.* **17** (1982) 2267.
10. R. J. CRAWFORD, *Polym. Eng. Sci.* **22** (1982) 302.
11. R. W. TRUSS, K. S. HAN, J. F. WALLACE and P. H. GEIL, *ibid.* **20** (1980) 747.
12. Hoechst Plastics, Hostalen GUR (PE-UHMW) datasheets, 6230 Frankfurt an Main 80.
13. BS 2782: Part 3: Method 341A.
14. H. S. LOVELESS, in "Testing of Polymers", vol. 2, edited by J. V. Schmitz (Interscience Publishers, New York, 1966) p. 321.
15. P. J. NEALE, K. L. ALDERSON, A. P. PICKLES and K. E. EVANS, *J. Mater. Sci. Lett* **12** (1993) 1532.
16. K. UMEYA and R. HARA, *Polym. Eng. Sci.* **18** (1978) 366.
17. K. S. HAN, J. F. WALLACE, R. W. TRUSS and P. H. GEIL, *J. Macromol. Sci. Phys.* **B19** (1981) 313.
18. K. L. ALDERSON and K. E. EVANS, *J. Mater. Sci.* **28** (1993) 4092.

*Received 22 August 1994
and accepted 10 October 1994*